Decision Feedback Equalization for Indoor Visual Light Communication

Namyong Kim

Abstract—In integrated systems of indoor visual light communication and power line communication technology, interference including multipath effect, DC bias and impulsive noise is a crucial obstacle to be coped with. In this paper, a recursive equalizer algorithm that can reduce the high computational complexity of blind decision feedback equalizer algorithms in order for advantages in implementation, and for the robustness against interference. The summation operation in the calculation of gradient of the cost function of the lagged cross-correlation of probability (LCCP) algorithm is transformed into a recursive gradient calculation. The proposed method reduces the computational burden of $O(N)$ to $O(1)$, which is independent of the data block size N. From the results of the simulation, the proposed method yielded the superior learning performance with reduced computation complexity.

Keywords—Recursive gradient, DF-LCCP, indoor VLC, DC noise.

I. INTRODUCTION

INDOOR wireless sensor data communication technologies optical wireless is in great demand due to its usability even in some RF-restricted areas such as hospitals or airplanes. In some optical wireless technologies, visible light communication (VLC) utilizes white LEDs as illumination with a long lifetime and energy efficiency, and at the same time as a transmitter of sensor information in a way that humans cannot perceive it by modulating the light intensity at high rates beyond that of human perception [1].

In indoor VLC systems, non-line-of sight (NLOS) links utilizing reflected paths of the light from indoor wall, ceiling and furniture have robustness to blocking, but suffer from multipath effect that results in intersymbol interference (ISI) in the received signal [2][3]. Furthermore, in the NLOS-VLC systems with white LEDs, background solar radiation and incandescent lamps play the role of main sources of DC bias noise, with which received signal is distorted seriously [4].

Recently, integration approaches of VLC systems combined with power line communication (PLC) systems are emerging for home sensor networking [5][6]. In the integrated systems, abrupt power surges on the PLC network can cause impulsive noise inducing burst error occurrence [6][7]. Therefore, the integrated sensor network systems of VLC and PLC

N. Kim is with the Kangwon National University, Samcheok, Korea (corresponding author : 82-33-570-6400; fax: 82-33-574-5300; e-mail: namyong@kangwon.ac.kr).

(VLC/PLC) should be equipped with devices that can compensate for multipath effect, DC bias and impulsive noise, to provide reliable sensor data transmission. For that purpose, a decision feedback equalizer algorithm has been proposed in [8]. The equalizer algorithm is based on a cost function of lagged cross-correlation between probabilities (LCCP) density functions [9]. The researchers developed the linear LCCP algorithm into its decision feedback version on the ground that error propagation problems can be avoided, since the Gaussian kernel of the linear LCCP has immunity against impulsive noise and the variable lag within the correlation function can deal with DC bias noise [8].

However, the weight update equation of the decision feedback LCCP algorithm using a block of output samples N contains the computations of $O(N)$ at each iteration time for each filter section. This computational complexity can prevent practical implementation. In this paper, a solution to reduction of the computational burden of the LCCP-DF algorithm is proposed and tested to see whether it produces the same weight update performance while keeping the reduction in the computational complexity.

II. INTERFERENCE IN VLC/PLC ENVIRONMENTS

The transmitted light signals in indoor VLC come to receivers through multipath channels that induce ISI. The ISI prevents the system from achieving high rate of sensor data transmission. The researchers in [3] gained information about the channel impulse response in their NLOS experimental setting of a transmitter and two receivers $Rx1$, field-of-view (FOV) 40° and $Rx2$, FOV=132°, in an empty typical office room. They found that ISI has a large influence on data rate performance from above 100 Mb/s, and the receiver with larger FOV is more prone to be affected by ISI. In this paper, the data rate of 150 Mb/s and FOV=132° are chosen for performance evaluation.

Sunlight and other illumination can affect VLC systems when light switches are turned on or off, and sunlight enters through opened curtains or blinds. This changing ambient light induces DC bias noise causing deterioration in detector sensitivity, requiring appropriate schemes for elimination of the DC bias noise component in the received signal [10] [11].

Another type of noise problem is observed in the integrated system VLC/ PLC. The wireless signal received from LED lighting can be retransmitted through the wired PLC network. Multiple appliances connected to the same power-line network generate noises which are impulsive. Impulsive noise is the

main source of interference that causes severe signal distortions, leading to bursts bit errors while transmitting data. Origins of impulsive noises can be domestic appliances such as power switches, power supplies, motors, power sockets, thermostats [12]. The impulsive noise model in this paper employs the model from [7] and [13] that is widely adopted in most PLC systems. The distribution function $f_I(n_{Im})$ of the random impulsive noise n_{Im} is expressed in (1) which is the same one in [8].

$$f_I(n_{Im}) = \frac{\varepsilon}{\sqrt{2\pi(\sigma_{GN}^2 + \sigma_{IN}^2)}} \exp[\frac{-n_{Im}^2}{2(\sigma_{GN}^2 + \sigma_{IN}^2)}]$$

$$+ \frac{1-\varepsilon}{\sigma_{GN}\sqrt{2\pi}} \exp[\frac{-n_{Im}^2}{2\sigma_{GN}^2}] \qquad (1)$$

where σ_{GN}^2 is the variance of background Gaussian noise and σ_{IN}^2 is that of impulse noise. Impulse noise occurs according to a Poisson process and the average number ε of impulses per information symbol duration. And an example of generated DC bias and impulsive noise according to the distribution model is given in Fig. 1.
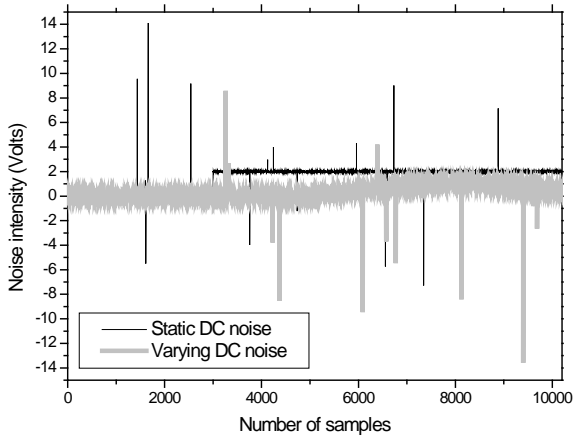
Fig. 1. Generated noise composed of background Gaussian noise, impulsive noise and two types of DC bias noise for simulation.

III. BLIND EQUALIZATION BASED ON THE LCCP CRITERION FOR VLC/PLC

Blind equalizer algorithms are widely used in multipath environments where training sequences for starting up or restarting after a communications breakdown are not required [14]. For blind equalization under DC bias noise, the LCCP function has been introduced in [9]. For two given probability functions $f_S(x)$ for a source symbol set and $f_Y(x+\tau)$ for output data at lag τ , the LCCP function is defined as $R_{SY}(\tau) = \int f_S(\alpha) \cdot f_Y(\alpha + \tau) d\alpha$.

For the basic binary modulation scheme OOK with NRZ pulses to VLC as in [3], the distribution function of transmitted symbols (+1, -1) can be $f_S(\alpha) = \frac{1}{2}[\delta(\alpha-1) + \delta(\alpha+1)]$. The probability function $f_Y(x)$ for output data can be constructed by kernel density estimation method with a Gaussian kernel $G_\sigma(x) = \frac{1}{\sigma\sqrt{2\pi}} \exp[\frac{-x^2}{2\sigma^2}]$ and N output samples $\{y_{k-N+1}, y_{k-N+2},..., y_k\}$ at current sample time k [15] as

$$f_Y(x) \cong \frac{1}{N} \sum_{i=k-N+1}^{k} G_\sigma(x - y_i) \cdot \qquad (2)$$

Then the LCCP function becomes

$$R_{SY}(\tau) = \frac{1}{2N} \sum_{i=k-N+1}^{k} [G_\sigma(1+\tau-y_i) + G_\sigma(-1+\tau-y_i)] \cdot \qquad (3)$$

Maximization of the LCCP function with respect to an adaptive system variable forces the system to produce output samples y_i concentrated on the transmitted symbol points +1 and -1. Defining a biased output $y_{biased,i}$ as $y_{biased,i} = y_i - \tau$ and biased error $s_j - y_{biased,i}$ as $e_{biased}(j,i)$, respectively, the LCCP function to be maximized is

$$R_{SY}(\tau) = \frac{1}{2N} \sum_{i=k-N+1}^{k} [G_\sigma(e_{biased}(1,i)) + G_\sigma(e_{biased}(-1,i))] \cdot \qquad (4)$$

The Gaussian kernel in the LCCP function (4) is a function of biased error and an exponential decay function, so that excessively large biased errors mostly induced by strong impulsive noise become negligible in the LCCP criterion. Furthermore, maximization process of the LCCP function (4) leads the biased error samples $e_{biased}(1,i)$ for symbol 1 and $e_{biased}(-1,i)$ for symbol -1 to become zero, which means the bias τ induced from the inflow of DC bias noise can be cancelled out as the amount of τ is adjusted in the system.

This property of canceling ISI, impulsive noise and DC bias noise makes it possible to prevent error propagation problems when decision feedback approach is employed.

.

.

IV. DECISION FEEDBACK LCCP ALGORITHM AND RECURSIVE GRADIENT CALCULATION

As will be observed in the simulation results, the linear LCCP algorithm is ineffective in data rates above 100 Mb/s rate from where ISI has a large influence on data rate performance. To improve data rate by way of residual ISI cancelation, decision feedback equalizer (DFE) schemes can be considered. The decision feedback structure is made up of the feed-forward section and feedback section. Feed-forward section with weight vector $\mathbf{W}_k^F = \left[w_{k,0}^F, w_{k,1}^F, w_{k,2}^F, ..., w_{k,P-1}^F \right]^T$ and input vector $\mathbf{X}_{k,P} = [x_k, x_{k-1}, x_{k-2}, ..., x_{k-P+1}]^T$ produces $y_k^F = \left[\mathbf{W}_k^F \right]^T \mathbf{X}_{k,P}^*$. And the output of feedback section with weight vector $\mathbf{W}_k^B = \left[w_{k,0}^B, w_{k,1}^B, w_{k,2}^B, ..., w_{k,Q}^B \right]^T$ and $\hat{\mathbf{D}}_{k-1} = \left[\hat{d}_{k-1}, \hat{d}_{k-2}, ..., \hat{d}_{k-Q-2}, c \right]^T$ is $y_k^B = \left[\mathbf{W}_k^B \right]^T \hat{\mathbf{D}}_{k-1}^*$, where c is a constant and $\hat{d}_k$ is the decided value of a decision device. Then the equalizer output becomes $y_k = y_k^F + y_k^B$.

The steepest ascent method using gradients $\dfrac{\partial R_{SY}(\tau)}{\partial \mathbf{W}^F}$ and $\dfrac{\partial R_{SY}(\tau)}{\partial \mathbf{W}^B}$ in maximization of (3) with respect to each weight vector yields the weight updating equations as

$$\mathbf{W}_{k+1}^F = \mathbf{W}_k^F + \mu_{LCCP} \frac{\partial R_{SY}(\tau)}{\partial \mathbf{W}^F} , \tag{5}$$

and

$$\mathbf{W}_{k+1}^B = \mathbf{W}_k^B + \mu_{LCCP} \frac{\partial R_{SY}(\tau)}{\partial \mathbf{W}^B} . \tag{6}$$

Defining
$$\nabla_k^F = \frac{\partial R_{SY}(\tau)}{\partial \mathbf{W}^F} , \tag{7}$$
and
$$\nabla_k^B = \frac{\partial R_{SY}(\tau)}{\partial \mathbf{W}^B} , \tag{8}$$

each gradient vector ∇_k^F and ∇_k^B can be written as

$$\nabla_k^F = \frac{1}{2\sigma^2 N} \sum_{i=k-N+1}^{k} [(1+\tau-y_i) \cdot G_\sigma(1+\tau-y_i) \\ + (-1+\tau-y_i) \cdot G_\sigma(-1+\tau-y_i)] \mathbf{X}_{i,P}^*. \tag{9}$$

and

$$\nabla_k^B = \frac{1}{2\sigma^2 N} \sum_{i=k-N+1}^{k} [(1+\tau-y_i) \cdot G_\sigma(1+\tau-y_i) \\ + (-1+\tau-y_i) \cdot G_\sigma(-1+\tau-y_i)] \hat{\mathbf{D}}_{i-1}^*. \tag{10}$$

It is noticeable that the gradient vectors ∇_k^F and ∇_k^B for the weight update at each iteration are calculated with the computations of $O(N)$ for each filter section. This computational burden can be an obstacle for practical implementation. In the following section a solution for reducing computational complexity of LCCP-DF algorithm is proposed by computing each gradient recursively, by utilizing the previously calculated gradient and current data.

In the initial state for the time $1 \le k \le N$, when a new sample y_k is obtained, we have k samples to estimate the gradient at time k. Therefore, each gradient vector can be expressed as

$$\nabla_k^F = \frac{1}{2\sigma^2 k} \sum_{i=1}^{k} [(1+\tau-y_i) \cdot G_\sigma(1+\tau-y_i) \\ + (-1+\tau-y_i) \cdot G_\sigma(-1+\tau-y_i)] \mathbf{X}_{i,P}^*. \tag{11}$$

and

$$\nabla_k^B = \frac{1}{2\sigma^2 k} \sum_{i=1}^{k} [(1+\tau-y_i) \cdot G_\sigma(1+\tau-y_i) \\ + (-1+\tau-y_i) \cdot G_\sigma(-1+\tau-y_i)] \hat{\mathbf{D}}_{i-1}^*. \tag{12}$$

Separation of the recent data at time k from each summation leads to

$$\nabla_k^F = \frac{(k-1)}{2\sigma^2 k(k-1)} \sum_{i=1}^{k-1} [(1+\tau-y_i) \cdot G_\sigma(1+\tau-y_i) \\ + (-1+\tau-y_i) \cdot G_\sigma(-1+\tau-y_i)] \mathbf{X}_{i,P}^* \\ + \frac{1}{2\sigma^2 k} [(1+\tau-y_k) \cdot G_\sigma(1+\tau-y_k) \\ + (-1+\tau-y_k) \cdot G_\sigma(-1+\tau-y_k)] \mathbf{X}_{k,P}^* \tag{13}$$

$$= \frac{(k-1)}{k} \nabla_k^F + \frac{1}{2\sigma^2 k} [(1+\tau-y_k) \cdot G_\sigma(1+\tau-y_k) \\ + (-1+\tau-y_k) \cdot G_\sigma(-1+\tau-y_k)] \mathbf{X}_{k,P}^*. \tag{14}$$

Similarly,

$$\nabla_k^B = \frac{(k-1)}{k} \nabla_k^B + \frac{1}{2\sigma^2 k} [(1+\tau-y_k) \cdot G_\sigma(1+\tau-y_k) \\ + (-1+\tau-y_k) \cdot G_\sigma(-1+\tau-y_k)] \hat{\mathbf{D}}_{k-1}^*. \tag{15}$$

In the state $k \ge N+1$, the last gradient for the feed forward section at time $k-1$ becomes

$$\nabla_{k-1}^F = \frac{1}{2\sigma^2 N} \sum_{i=k-N}^{k-1} [(1+\tau-y_i) \cdot G_\sigma(1+\tau-y_i) \\ + (-1+\tau-y_i) \cdot G_\sigma(-1+\tau-y_i)] \mathbf{X}_{i,P}^*. \tag{16}$$

The last gradient for the feedback section at time $k-1$ is

$$\nabla_{k-1}^B = \frac{1}{2\sigma^2 N} \sum_{i=k-N}^{k-1} [(1+\tau-y_i) \cdot G_\sigma(1+\tau-y_i) \\ + (-1+\tau-y_i) \cdot G_\sigma(-1+\tau-y_i)] \hat{\mathbf{D}}_{i-1}^*. \tag{17}$$

By separating the current data at time k and the old data at time $k-N+1$ from the current gradient vectors ∇_k^F and ∇_k^B we have

$$\nabla_k^F = \frac{1}{2\sigma^2 N} \sum_{i=k-N}^{k-1} [(1+\tau-y_i) \cdot G_\sigma(1+\tau-y_i) \\ + (-1+\tau-y_i) \cdot G_\sigma(-1+\tau-y_i)] \mathbf{X}_{i,P}^*$$

$$+[(1+\tau-y_k)\cdot G_\sigma(1+\tau-y_k)$$
$$+(-1+\tau-y_k)\cdot G_\sigma(-1+\tau-y_k)]\mathbf{X}^*_{k,P}$$
$$-[(1+\tau-y_{k-N})\cdot G_\sigma(1+\tau-y_{k-N})$$
$$+(-1+\tau-y_{k-N})\cdot G_\sigma(-1+\tau-y_{k-N})]\mathbf{X}^*_{k-N,P}. \quad (18)$$

That is

$$\nabla^F_k = \nabla^F_{k-1} +[(1+\tau-y_k)\cdot G_\sigma(1+\tau-y_k)$$
$$+(-1+\tau-y_k)\cdot G_\sigma(-1+\tau-y_k)]\mathbf{X}^*_{k,P}$$
$$-[(1+\tau-y_{k-N})\cdot G_\sigma(1+\tau-y_{k-N})$$
$$+(-1+\tau-y_{k-N})\cdot G_\sigma(-1+\tau-y_{k-N})]\mathbf{X}^*_{k-N,P}. \quad (19)$$

Accordingly

$$\nabla^B_k = \nabla^B_{k-1} +[(1+\tau-y_k)\cdot G_\sigma(1+\tau-y_k)$$
$$+(-1+\tau-y_k)\cdot G_\sigma(-1+\tau-y_k)]\hat{\mathbf{D}}^*_{k-1}$$
$$-[(1+\tau-y_{k-N})\cdot G_\sigma(1+\tau-y_{k-N})$$
$$+(-1+\tau-y_{k-N})\cdot G_\sigma(-1+\tau-y_{k-N})]\hat{\mathbf{D}}^*_{k-N-1}. \quad (20)$$

The initial gradient vectors ∇^F_0 and ∇^B_0 are set to 0.

We can notice that the resulting recursive expressions (14) and (15) for $1 \le k \le N$, and (19) and (20) for $k \ge N+1$ reduce the computational complexity $O(N)$ in (7) and (8) to $O(1)$, which is independent of the data block size N and more appropriate to practical implementations.

V. RESULTS AND DISCUSSIONS

To investigate whether the proposed recursive approach of (19) and (20) produces the same gradient values as the original gradients (7) and (8) which are calculated by the block processing method, gradient values for various data-block size N are tested under the same experimental environment as in [8].

The gradients of the equalizer taps (the first and second tap are chosen for convenience's sake) with $N=20$ are depicted in Fig. 2 for the first tap's gradient and Fig. 3 for the second tap's gradient. We can notice that though the trace of gradient for each method is different in the initial state where the memory for the summation is not fully occupied, the two curves come close to each other as the iteration increases. More importantly, we observe the two curves become identical after the iteration number 20, when the memory for the summation is full. To verify this phenomenon, the same experiment has been carried out for $N=40$ and the results are shown in Fig. 4 for the first tap and Fig. 5 for the second tap.
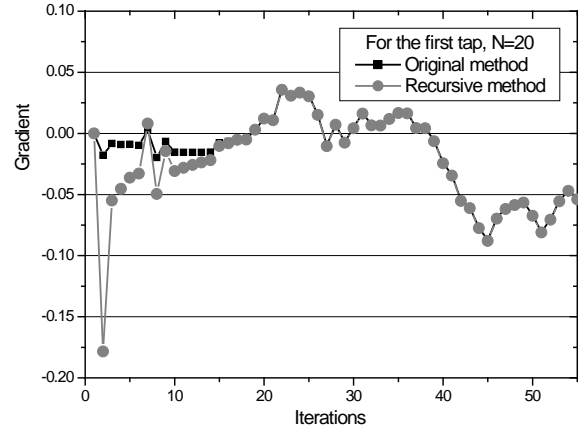
Fig. 2. Learning curves for the first tap with the data block size $N=20$.

In accordance with our expectation, the proposed method yields in the case of $N=40$ the same gradient values as the original block processing method for any equalizer tap after iteration number 40. These results indicate that the proposed recursive method produces the same performance as the original method and its computational complexity is independent of the data block size N whereas the original one is heavily dependent.
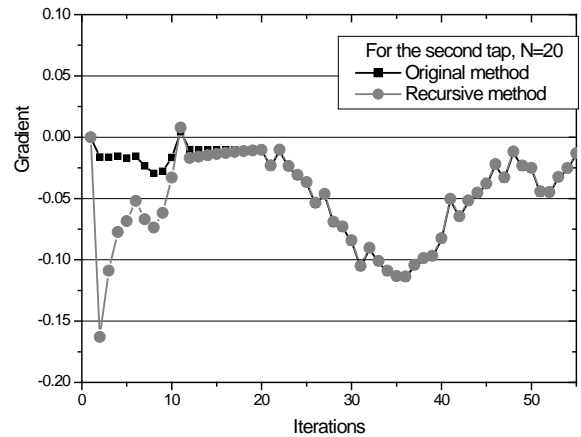
Fig. 3. Learning curves for the second tap with the data block size $N=20$.
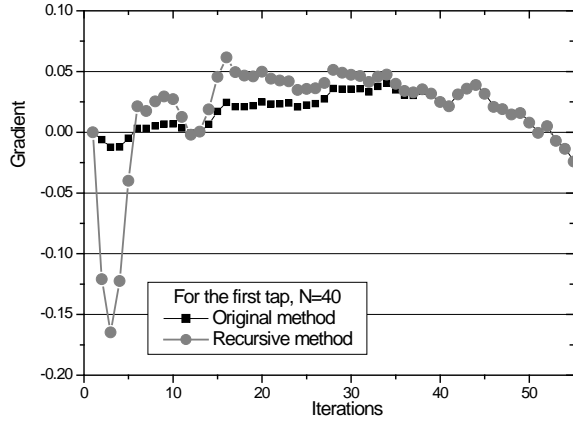
Fig. 4. Learning curves for the first tap with the data block size $N = 40$.
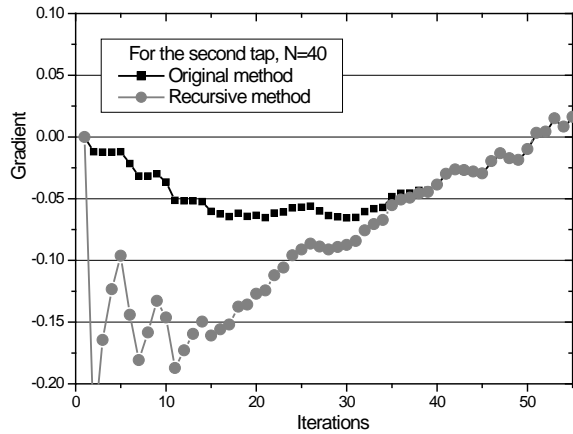
Fig. 5. Learning curves for the second tap with the data block size $N = 40$.

For evaluation of MSE convergence performance we selected another impulse response of NLOS links in VLC systems as follows. The normalized impulse response for this experiment was obtained from the measurements taken in an empty typical office room, with a transmitter and two FOV receivers $Rx1$ ($40°$) and $Rx2$ ($132°$) [3]. The transmission speed is 150 Mbps. The z-transform of the impulse response is

$$H(z) = 0.1478 + 0.7540z^{-1} + 0.5737z^{-2} + 0.2455z^{-3}$$
$$+ 0.1217z^{-4} + 0.0674z^{-5} + 0.0282z^{-6} + 0.0087z^{-7} \quad (21)$$

The transmitted symbol points are binary $\{+1,-1\}$ as in [3] for VLC. The random impulsive noise and DC bias noise as in Fig. 2 is added to the received signal. The parameters for the impulsive noise model are $\varepsilon = 0.0012$, $\sigma_{GN}^2 = 0.001$, $\sigma_{IN}^2 = 50$. In the case of static DC noise, DC 2V is added to the background Gaussian noise from the sample number 3000. In the case of varying DC noise, $\sin(2\pi k / 5000)$ is started to be added from $k = 5000$ as depicted in Fig. 1. The feed forward filter length is $P = 11$ and the backward filter length is $Q = 4$. The linear filter length is the sum of P and Q as $L = 15$. The kernel size is $\sigma = 0.6$ and the data-block size is $N = 20$. The same convergence parameter $\mu_{LCCP} = 0.01$ is used as in [8]. Decision feedback algorithms are compared with linear algorithms for performance evaluation. DF and linear correntropy algorithms are also compared since they were developed based on the generalized correlation function in a kernel-transformed space and are well known to have impulsive noise immunity [13]

In Fig. 6 and 7, MSE convergence performance is compared under impulsive noise for all the sample time and DC bias noise starts to be added at the sample time 3000. The linear and DF version of the correntropy algorithm suffer from DC bias noise and impulsive noise under the NLOS/VCL channel, showing a very slow convergence. On the other hand, linear and DF version of LCCP algorithm show rapid learning curves from the start. After DC noise addition, the recursive DF_LCCP converges within 1000 samples reaching -28 dB while the linear version reaches -13 dB of steady state MSE. The 15 dB performance gain in the environment of FOV=132° and 150 Mbps speed indicates that DF-LCCP employing the recursive gradient calculation can enable the VLC system to achieve highly reliable sensor data transmission at higher data rate even under the interference of various ambient light changes and electrical sparks from the combined PLC medium.

In the comparison of MSE convergence performance under impulsive and slowly varying DC bias noise as in Fig. 7, the correntropy based algorithms fail to achieve cancellation of varying DC noise, on the other hand, the recursive DF-LCCP algorithm shows no perturbation from varying DC noise, yielding -28 dB of steady state MSE.

For clearer observation of the compensation capability against multipath, impulsive and static DC bias noise, the output samples of the DF-LCCP are depicted in Fig. 8. It is noticed that output samples are quickly returned to the symbol points -1 and 1 after the time 3000 when DC bias is added and are kept in highly concentrated state. The outlying random dots represent output samples when impulsive noise is present, but we see they do not influence the weight updating equations of the DF-LCCP algorithm producing stable output samples after the impulses.
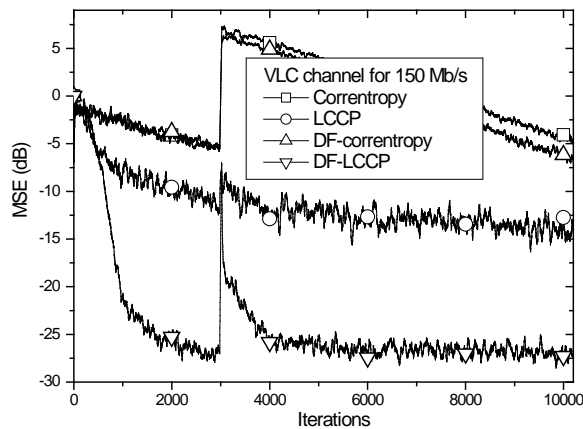
Fig. 6. MSE convergence performance under impulsive and static DC bias noise.
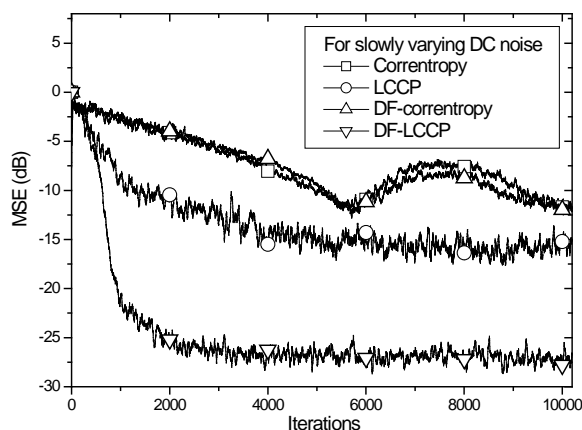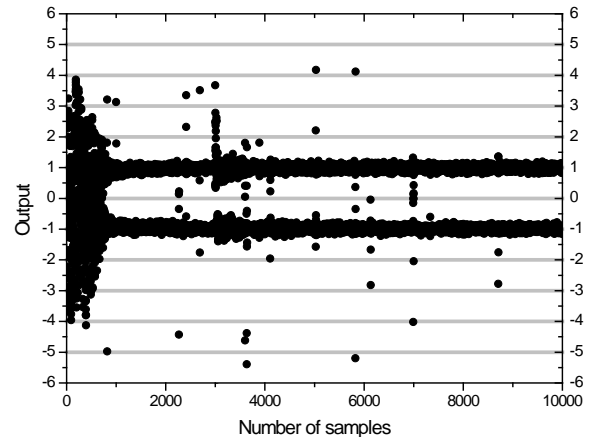
Fig. 8. The convergence of output samples of DF-LCCP.

VI. CONCLUSION

Indoor visual light communication technology is in great demand where the white LEDs for energy saving illumination are used as transmitters for indoor sensor networks. In recent integrated VLC/PLC systems multipath effect, DC bias and impulsive noise are problematic obstacles. In this paper, for the purpose of robustness against interference, and for advantages in implementation, a recursive method is proposed for reducing the computational complexity of blind decision feedback equalizer algorithms. Through investigation of the summation properties in the calculation of the feed-forward and feedback gradient of DF-LCCP algorithm, a recursive gradient calculation method was derived. The method reduces the computational burden of $O(N)$ to $O(1)$, which is independent of the data block size N. From the results of the simulation, the proposed method yielded superior learning performance, but with reduced computational complexity. This indicates that the proposed recursive method of the gradient calculation of the decision feedback LCCP equalizer algorithm has the capability of compensation for multipath effect, impulsive and DC bias noise in the indoor VLC/PLC environment and is more appropriate for practical implementations.

Fig. 7. MSE convergence performance under impulsive and slowly varying DC bias noise.

REFERENCES

[1] http://www.comsoc.org/files/Publications/Magazines/ci/cfp/cfpcommag 1213.htm

[2] J. Carruthers, S. Carroll, and P. Kannan, "Propagation modelling for indoor optical wireless communications using fast multi-receiver channel estimation," Optoelectronics, IEE Proceedings, vol.150, pp. 473 – 481, Oct. 2003.

[3] Z.Dong, K. Cui, G. Chen, and Z. Xu, "Non-line-of-sight link performance study for indoor visible light communication systems," Proc. of SPIE Photonics and Optics – Free Space Laser Communications IX,San Diego, CA, pp. 781404-1-781404-10, August 2010.

[4] K. Cui, G. Chen, Z. Xu, and R. Roberts, "Line-of-sight visible light communication system design and demonstration," Proc. of CSNDSP 2010, Newcastle, Tyne, pp. 621-625, July, 2010.

[5]   H. Lee, Y. Kim, and K. Sohn, "Optical wireless sensor networks based on VLC with PLC-Ethernet interface,"World Academy of Science, Engineering and Technology, vol. 57, pp. 245-248, July, 2011.

[6]   S.Alavi, A.Supaat, S.Idrus, S.Yusof,"Integrated system of visible free space optic with PLC," Proc. of MICC 2009, Kuala Lumpur, Malaysia, pp. 271-275, Dec. 2009.

[7]   N. Andreadou, and F. Pablidou, "PLC channel: impulsive noise modelling and its performance evaluation under different array coding schemes," IEEE Trans. Power Delivery, vol. 24, pp. 585-595, April. 2009.

[8]   N. Kim and H. Byun, "Indoor sensor data transmission for energy-saving buildings", Proc. of ESPCO 2013, Venice, Italy, pp. 71-75, Sep. 2013.

[9]   N. Kim, K. Kwon and Y, You, "Lagged cross-correlation of probability density functions and application to blind equalization," JCN, vol. 14, pp. 540-545, Oct. 2012.

[10] M. Saadi, L. Wattisuttikulkij, "Visible light communication : opportunities,   challenges   and   channel models,"http://www.cennser.org/IJEI/eiV02N01 /ei020101.pdf.

[11] J. Choi, "Performance analysis of the VLC system with Z-HBT line coding," Proc. of ISCIT 2009, Icheon, Korea, pp. 1242-1246, Sep. 2009.

[12] H. Chaouche, F. Gauthier, A. Zeddam, M. Tlich, and M. Machmoum, "Time domain modeling of powerline impulsive noise at its source,"Journal of Electromagnetic Analysis and Applications, vol. 3, pp. 359-367, Sept. 2011.

[13] I. Santamaria, P. Pokharel, and J. Principe, "Generalized correlation function: Definition, properties, and application to blind equalization," IEEE Trans. Signal Processing, vol. 54, pp. 2187-2197, June 2006.

[14] C. Johnson Jr., "Blind Equalization Using the Constant Modulus Criterion: A Review," in *Proc. of the IEEE*, vol. 86, pp. 1927–1950, Oct. 1998.

[15] E. Parzen, "On the estimation of a probability density function and the mode," *Ann. Math. Stat.* vol. 33 p. 1065, 1962.